CASE STUDY ABOUT RESISTANCE PROJECTION WELDING OF ALUMINIZED STEEL PARTS

I. Voiculescu*, V. A. Oprea, I. M. Vasile

University Politehnica of Bucharest, Faculty of Industrial Engineering and Robotics
313 Splaiul Independentei St., Sector 6, 060042 – Bucuresti, Romania
*Corresponding author's e-mail address: ioneliav@yahoo.co.uk

ABSTRACT

Resistance projection welding is a non-polluting mechanized process used to obtain an assembly between similar or dissimilar metallic materials. The main advantages of this welding process are the possibility to achieve many different welded points at the same time and the long life of the electrodes compared to the spot-welding process. The paper analyses the effects of thin aluminium coating existing on mild steel parts of on the correct formation of welding points when assembling moulds for the manufacture of baking bread. From optical and electron microscopy analyses it resulted that some adjacent welded points show an interrupted fusion line, sprinkled with elongated islands of aluminium-rich compounds. The paper presents the effect of changing the values of the welding parameters on the weld spot size, in correlation with the Al-rich inclusions that appear on the weld fusion zone. The best results have been obtained when the welding parameters values were the follows: electrode pressure of 2.6 bar, welding power of 19.18kVA and welding time of 7ms. The problems that occur when electric resistance welding of parts with aluminium coating have been highlighted, being useful for specialists who make products using this welding process.

KEYWORDS: projection welding, aluminium coating, microstructure.

1. INTRODUCTION

The projection welding process is derived from the general scheme of spot resistance welding, with the difference that the joint areas have provided some contact points obtained by local deformation of the surface (projections) to concentrate the current lines during welding [1] – [3]. Spot resistance welding is mainly used for thin sheet metal welding having the same thickness, while projection welding can also be applied to components with different thicknesses.

In projection welding (Fig. 1), the components to be welded (1 and 2) are pressed with force *P* by means of the flat surface electrodes (4 and 5), connected to the secondary of the low voltage electrical transformer (6). In the contact area of these protrusions a concentration of electric current and pressing force is obtained. In the first stage the protrusions, and areas adjacent to the contact between the protrusion tips are fast heated. When the melting temperature is reached in this contact area, due to the decrease of the yield strength of the materials, the protrusions flatten under the influence of pressure force P, and the welding continues to be carried out similarly to spot welding [3].

The joint will contain several welding points, located on the protrusions made on one of the components. Obtaining quality joints is conditioned, first, by a careful performing of the protrusions and by ensuring the optimal cleaning of the surfaces, so that the welding current and the pressing force are distributed as evenly as possible on the protrusions.

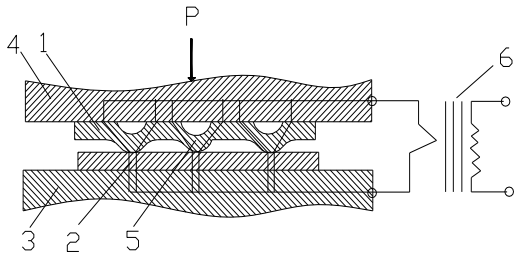

Fig. 1. Schematic of resistance projection welding process: 1 - upper sample with projections; 2 - flat sample; 3 and 4 - lower and upper electrodes of the pressing device; 5 - projection made by cold deformation; 6 - power supply for welding

When welding several projections at the same time, problems may occur in the equal distribution of current and heat, which can cause uneven flattening of the protrusions. Such problems can be avoided by

© *Galati University Press, 2021*

Date of submission/acceptance: 09.10.2021/15.12.2021 https://doi.org/10.35219/awet.2021.03

setting the optimal distance between the projections (to four times their diameter). Usually, the projection shape and height (0.5 to 1.5mm) are established based on the material thickness, elongation, and yield strength [3], [4]. In projection welding the nut leg geometry is decisive for the joint resistance (the optimum value is less than 0.2mm) [4]. Due to the fast decrease in the yield strength value of the material during heating, many tests are required to adjust the right values of the welding parameters [5]-[7]. The surface preparation of the samples before welding is an important factor that affects the weld quality. Any contaminant, like grease and oxide pellicles dramatically affect the resistance of the contact area between pieces [7], [8].

The electrode material must have a very good electrical conductivity to minimize overheating of the contact area between it and the parts to be welded. Although copper is the preferred metal, Cu-Cr or Cu-Cr-Be alloys are sometimes used to increase the compressive strength of the electrode [9] - [12]. In some works [9], [10] have been reported that to increase the durability of electrodes for electric resistance welding, a composite matrices by incorporating tungsten carbides into copper matrices can be used.

A feature of projection welding is the ability to quickly remove coating layers from the surface, allowing direct exposure of the two metals to form welded nugget. This aspect is beneficial because often the coating material can diffuse in the weld and forms compounds that diminish the mechanical resistance.

An example is the welding of galvanized steel, when the rapid evaporation of zinc causes the formation of pores in the weld. Another issue occurs when welding parts made of different materials, such as steel and aluminum, or when welding aluminum-plated steel sheets [12]-[14].

Reported studies have shown that if the welding current increases from 4 to 11 kA and the welding time increases from 50 to 300 ms, the diameter of the welded nugget increases [12], causing the coarse grains formation and cracks at the interface of the joint [15]. In these situations, weaker adhesion values and cracks in the weld were reported, by weakening the grain boundaries due to intermetallic compounds (Fe_2Al_5 and Fe_4Al_{13} phases) formation [15] - [18].

Aluminizing is a thermo-chemical diffusion process carried out at high temperatures, typically in the range of 800–1000°C, where the surface layer of the material is impregnated with aluminium. Using powder pack method, the temperature for aluminizing can decrease to 550^{o}C. It is primarily used on steels, but also on nickel and cobalt based alloys to obtain greater creep resistance, hardness, and corrosion resistance. During welding, the aluminized coating may suffer various changes in thickness, effects of vaporization and expulsion from surfaces, as well as cracks or exfoliation [19]. For this reason, welding of aluminized parts requires more tests than uncoated ones.

The paper analyzes the effect of welding parameters on the weld interface obtained by resistance projection process. The welded parts were made of aluminized steel sheet having different thickness. Since 3 points were made at the same time, their dimensions are analyzed comparatively. The geometry of the welded areas with different values of the welding parameters are analyzed, with the highlighting of the chemical elements concentration and associated phenomena due to intermetallic compounds that apears on the weld interface.

2. MATERIAL AND METHODS

In the research program, aluminized steel parts were welded using a TECNA 8005D Series Spot and Projection Welder machine (maximum welding power of 200 kVA, maximum welding current for steel of 28kVA). The flat-faced electrode with the working surface of 25x25mm was used for experiments.

The microstructural analysis was performed by optical microscopy, using the Olympus GX51 microscope equipped with specialized software for image processing (AnalySis) and by scanning electron microscopy using the Inspect S microscope equipped with Z2e EDAX AMETEC sensor.

The microhardness testing was performed with the Shimadzu HMV 2T equipment in the following conditions: temperature +25°C (reference temperature +23 ±5°C) and 55% humidity. The micro-hardness was measured on the cross section of the welded samples, applying the indentation load of 0.2 N and the indentation time of 10s.

The shear strength of welded samples was measured using tensile / compression test "W + b" Walter + bai ag testing machine, Switzerland. For this test, test samples with a width of 32 mm and a length of 150 mm were performed. On these samples, 3 protrusions were made simultaneously, with the same dimensions (depth and diameter). The samples were superimposed on a length of 32 mm and then were welded using the values of the established regime parameters.

To study he microstructure and to measure the microhardness on the welded area the welded spots were cut using high precision cutting machine IsoMet 4000. The cross-section areas were hot incorporated into the conductive resin (Fig. 2), and then were subjected to rough grinding using successive abrasive grit paper (400, 600, 800, 1000 and 1500). The final stage of metallographic preparation was polishing with alpha alumina powder having grain sizes from 3 to 0.1 μm. For highlighting microstructural characteristics (grain size and phase characteristics, weld interface imperfections and welding line measuring) polished surfaces were etched by specific metallographic agents (Nital 4%).

Fig. 2. Welded samples prepared for microstructure analyse

3. EXPERIMENTAL PART

The projection welding process was used to obtain the moulds for baking bread. For this purpose, a set of 8 moulds, with a wall thickness of 0.8 mm, were assembled on 2 parallel rows, being reinforced using a strip having 1.2 mm thickness and 32 mm width. Three protrusions were made on the thinner-walled parts, at relatively equal distances of about 10 mm, to ensure three-point contact with the stiffening strip. (Fig. 3).

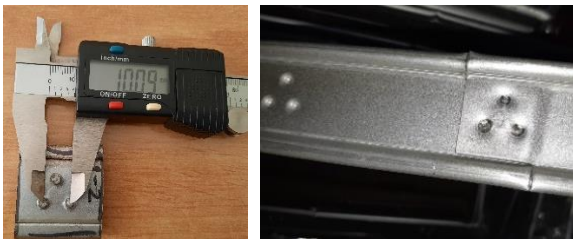

Fig. 3. Measurement of spot distance and detail on the projection welded sample

A recommended number was chosen for the welded points simultaneously (three), to obtain a safe contact between the two surfaces of the welded parts. The three main factors of the projection welding regime are studied: the pressing force, the electric power, and the welding time.

The pressing force should be set to only achieve a small deformation at the tip of the protrusion before the current pass through the joint. Then the force can be kept constant throughout the welding period or can be slightly increased in the last part of the process, to provide a forging effect.

For low power values and short welding times, the shear strength of the welds is low. Excessive heating and melting of the material may result in high power values and too long holding time during welding, which may cause the sample wall to be excessively deformed or perforated [1], [20].

The value of the pressing force at the beginning of the process was different for the three types of regimes analysed. If the value of this parameter is too high, the projection flattens rapidly before the welding point is formed. In this way, the contact surface is increased and the current density is reduced, limiting the amount of locally concentrated heat and the formation of a molten core with discontinuous or insufficient section to assure the required shear resistance. To study the effect of the values of the welding parameters, welds were made with different values of them, which are presented in table 1.

Table 1. Projection welding parameters

Sample	Electrode pressure [bar]	Pressure time [ms]	Welding time [ms]	Welding power [kVA]
1.1	2.8	10	7	19.81
1.2	2.6	10	7	19.18
2.2	3.4	10	5	18.10

4. RESULTS AND DISSCUSION

The pieces from this study were fabricated by rolled aluminized steel sheet. Aluminium-coated steel is widely used in the manufacture of baking dies. The thin layer of food grade aluminium improves corrosion resistance and makes it easier to extract products from baking moulds. The optical analyse of the microstructure of the aluminized steel surface indicates alpha aluminium dendritic formations and interdendritic compounds formed between the alloying elements (Fig. 4a).

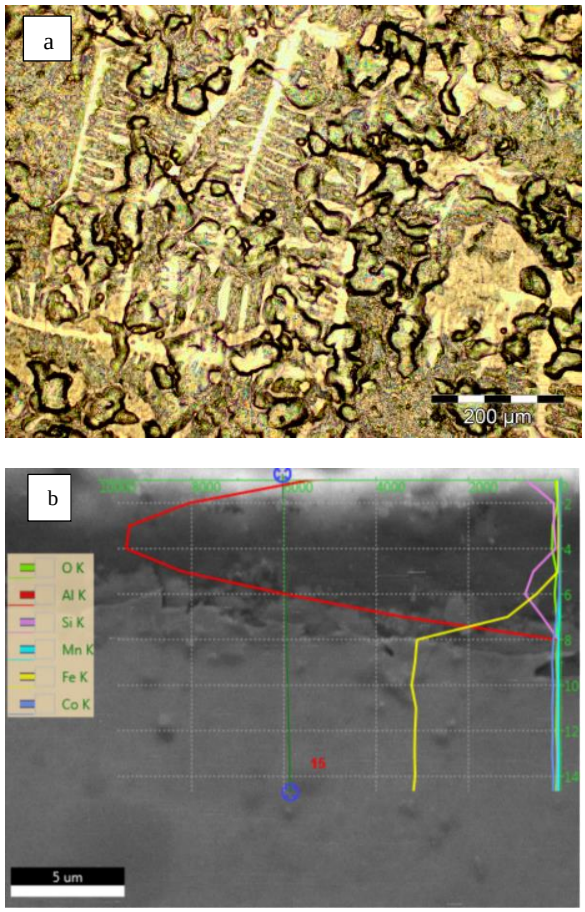

Fig. 4. The microstructure and chemical element analysis of aluminized steel surface

According to the EDS analyse performed on the aluminized steel sheet surface (Fig. 4b), the chemical composition contains (wt.%): 79.31 Al; 11.96 Si; 2.04 Fe; 0.34 Cr; 0.40 Ca; 5.96 O. Elements such as Ca and O can also come from the working atmosphere in which the samples have been exposed for a period of operation of about 6 months.

The evolution of the concentration of main chemical elements in the vicinity of the aluminized layer (Fig. 4b) shows a lower aluminium concentration at external surface level (due to formation of aluminium oxide and Al-Si compound), then increases in the middle area of the aluminized layer and begins to decrease towards the interface with steel sheet. At the same time, the diffusion of iron in the aluminized layer is observed, with the formation of the hard compound Al-Fe [17], [21] - [22].

In the detailed image of cross section of sample 1.1 (Fig. 5), is visible the aluminized layer that is composed by a thin bonding layer, BL (of about 5 microns thickness) located at the interface between the steel component and the aluminized layer (AL) (of about 20 microns thickness). Along of the bonding layer, chemical composition contains (wt.%): 1.22 Al; 0.94 Si; 96.29 Fe; 1 Co; 0.54Cu.

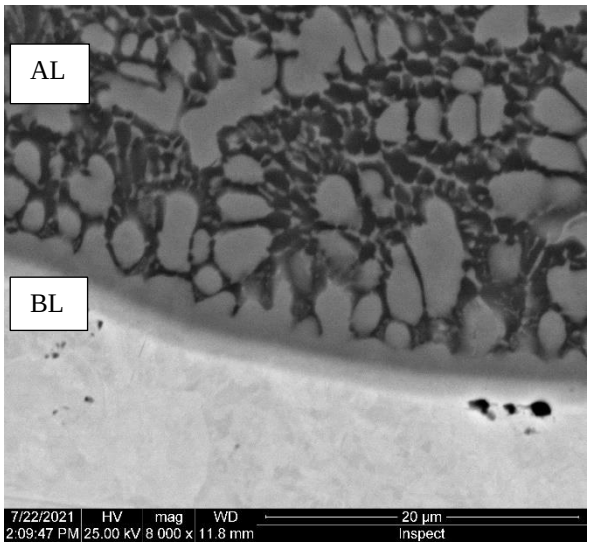

Fig. 5. The microstructure of aluminized layer (sample 1.1)

To study the weld geometry, some analyses were performed in cross section through the welded points. The aspects of the cross section for the samples joined using different values of welding regime parameters are shown in Fig 6.

Figure 6a corresponds to sample 1.1. which has the welding interface sprinkled with small discontinuities containing inclusions of Al-Si compounds. The total length of the interface (Table 2) is the largest of all the samples analysed, which also explains the higher value of the shear strength. Above the welded point, a thickening of the aluminium layer of 160 µm is observed.

Accumulations of compounds resulted by the detachment of aluminium oxide layer and the accumulation of impurities on the workpiece surfaces during welding have been largely expelled to the side areas of the weld. Small compounds are visible as elongated islands (of 2-10µm length) sprinkled on the molten nugget fusion line. The effective diameter of the welded area consists of annular portions with good adhesion alternating with small, detached areas at both ends of the molten core.

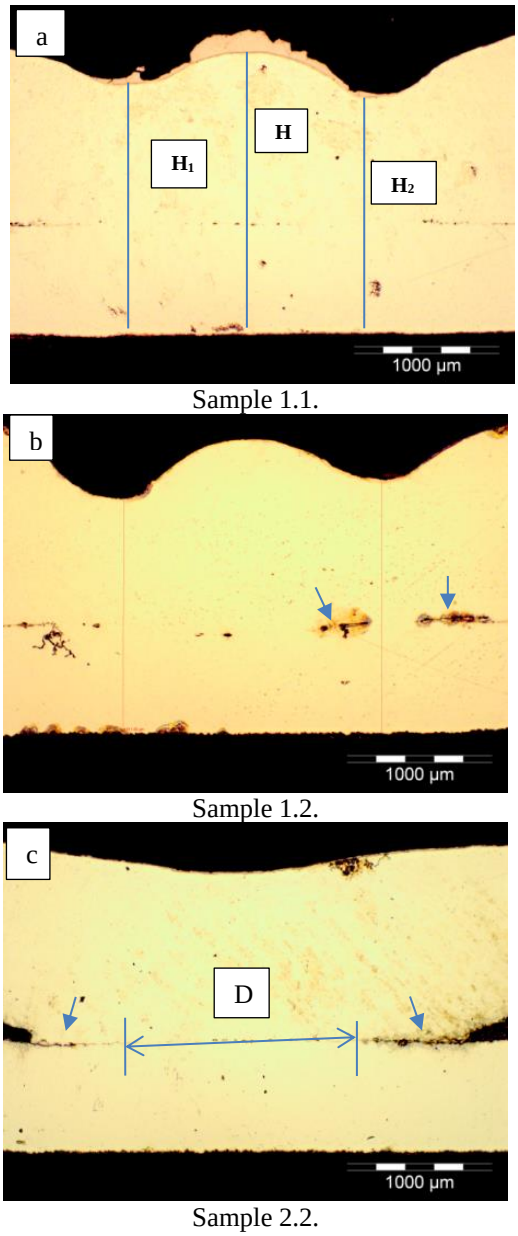

Fig. 6. Cross sections of projection welded samples

Table 2. Weld dimensions in cross-section

Sample	H [mm]	H_1 [mm]	H_2 [mm]	Weld diameter D [mm]
1.1	1.955	1.783	1.697	3.125
1.2	2.108	1.611	1.757	2.603
2.2	1.923	-	-	1.528

In the case of sample 1.2, the aluminized layer did not undergo obvious changes in thickness compared to sample 1.1 (Fig. 6b). However, small accumulations (see arrows) of it can be observed on the marginal areas of the weld molten nugget (Fig. 7).

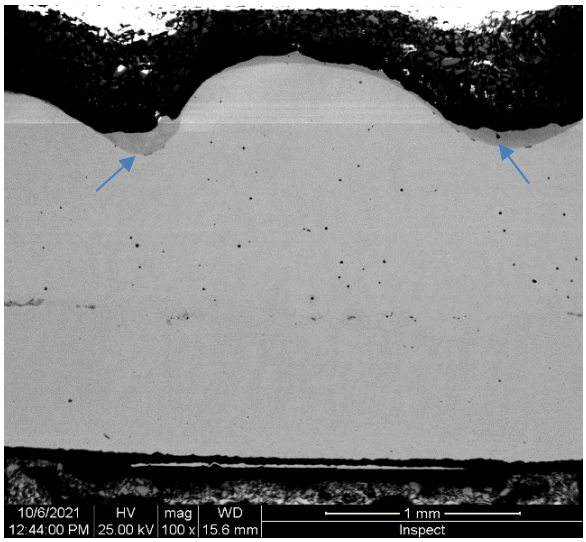

Fig. 7. Al-rich crust on the weld point for sample 1.2

Sample 2.2 (Fig. 6c) has a completely different appearance from the others, because it does not show prominence on the area of the welding point, but only a slight flattening. The length of the fusion line in this case is the shortest. At its ends there are accumulations of compounds expelled from the aluminized layer (Fig. 8).

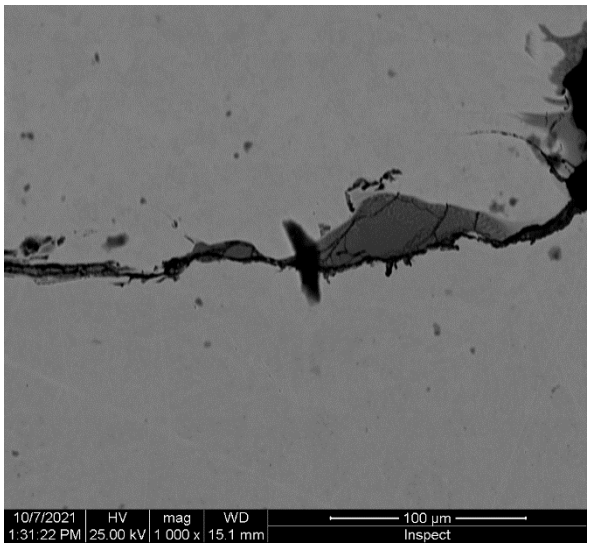

Fig. 8. Compounds located at extremities of weld nugget

EDS analysis of the chemical composition performed on the inclusions accumulated on the fusion line (Fig. 11) highlighted the presence of some compounds that contain (wt. %): 43-44 Al; 0.65-4 Si; 0.5 O; 1-1.2 Co; 0.3-0.4 Mn and Fe balance (Fig. 9).

The size of these inclusions (250 µm height and 500 µm length) is much larger in this sample compared to those identified in previous samples (20-50 µm).

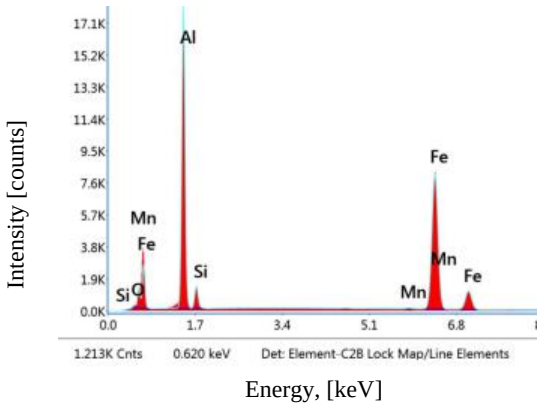

Fig. 9. EDS analyse of inclusion from fusion line for sample 2.2

These imperfections have determined the premature yielding of the baking forms during their exploitation at temperatures between 180-200ºC.

During welding, on the area of the welding point, the aluminium alloy layer was first melted, and then solidified rapidly. Therefore, the contraction stresses generated by this process caused cracking or rupture of the protective layer, thus exposing the uncovered steel area to corrosion in the working environment (hot oil, steam, temperatures of about 180-200ºC).

To assess the shear strength of the welded points, the samples were subjected to the tensile test. Shear loading of the single point can be calculated using the relation 1:

$$\tau = \frac{4F}{\pi D^2} \quad (1)$$

where F is breaking force and D is the welded spot diameter. For sample 1.1, value of τ was of 208.7 MPa. The appearance of the detached points during the shear test is shown in figure 10 (a - upper surface; b - lower surface).

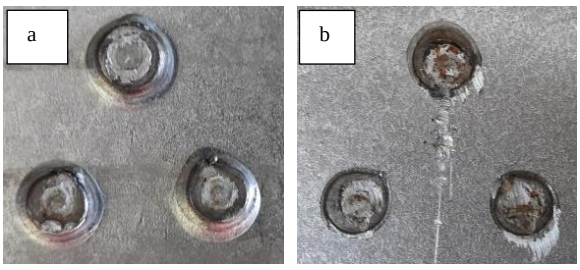

Fig. 10. Aspect of tearing surfaces after shear test

Examining the fracture surfaces although they were made simultaneously, the sections of the welding points are not equal and perfectly circular. This may be due to wear of the electrode surface,

which does not press with equal pressure on all 3 protrusions, incorrect positioning of the sample, incorrect deformation of projections or thermal imbalance that is generated in the joint by electric shunting of coated steel.

To avoid the unwanted effect of altering the aluminium coating, the values of electric power during welding (from 19.81 kVA to 19.18 kVA) and the electrode pressure (from 2.8 bar to 2.6 bar) were slightly reduced in the case of sample 1.2. The immediate consequence of this change in the values of the welding parameters was the preservation of the integrity of the protective layer both on the deformed area and on the flat area of the melting point. However, a good expulsion of the inclusions of compounds from the welding fusion line was not obtained, which reduced the effective diameter of the welding point and implicitly its shear strength (τ = 183.2 MPa). In the case of the sample 2.2, the welding time was reduced to 5 ms and the value of the electrode pressure was increased to 3.4 bar.

At the same time, it was necessary to reduce the electric power to diminish the effect of rapid flattening of the projection spot. The change of the values of welding parameters was not beneficial in this case, as the diameter of the weld point was reduced by half compared to the case of sample 1.1, proportionally reducing the value of the shear strength (to 103.2 MPa). At the same time, non-adhesion zones were formed at both ends of the molten core, filled with accumulated oxides and inclusions (Fig. 8).

The microhardness has been measured on base material, fusion line and heat affected zone (HAZ) and the values are presented in table 3.

Table 3. Microhardness of welded samples

Sample/ measuring zone	Individual value, $HV_{0.2}$	Average value, $HV_{0.2}$	Standard deviation	Coefficient of variation
Base material	155, 152, 158, 156, 157	156	2.30	1.48
Sample 1.1				
Aluminized layer	870, 856, 864, 864, 851	861	7.48	0.87
Fusion line	193, 187, 184, 190, 185	188	3.70	1.97
HAZ	161, 158, 165, 155, 153	158	4.77	3.01
Sample 1.2				
Fusion line	190, 185, 188, 183, 181	185	3.65	1.97
HAZ	160, 152, 160, 158, 155	157	3.46	2.21
Sample 2.2				
Fusion line	178, 170, 179, 178, 176	176	3.63	2.06
HAZ	152, 155, 153, 159, 153	154	2.79	1.81

The very high value of the hardness of the aluminized layer located above the welding point (861 $HV_{0.2}$) is due to the formation of their strong Al-Fe compounds, because the iron diffuses from the steel sheet during welding. Following the measurements of the chemical composition on the micro-area adjacent to the aluminized layer, a concentration of 2wt.% Fe was determined.

The hardness on the welding line (188, 185 and 176 $HV_{0.2}$) is about 20% higher compared to the base material (156 $HV_{0.2}$). This value can be influenced both by the higher cooling rate in the welding area and by the presence of hard Al-Fe compounds resulting from the aluminized layer.

This explanation is also supported by the low hardness values in HAZ, compared to the fusion line, but very close to those of the base material.

In sample 2.2, the amount of heat developed by the resistive effect was lower, which led to a reduction in hardness in both the welded area (176 $HV_{0.2}$) and the HAZ (154 $HV_{0.2}$).

5. CONCLUSIONS

Obtaining welded joints with appropriate characteristics between aluminized steel components requires the correct choice of the values of the regime parameters and performing of several mechanical tests to validate the welding technology.

If the value of the pressing force is directly correlated with the welding power and time, it is possible to remove completely the aluminium coating from the weld point area.

Of the 3 types of projection welding regimes analysed on paper, the corresponding values for the parameters corresponding to the following ranges: electrode pressure between 2.6 bar and 2.8 bar, welding time of 7 ms and power between 19.81 and 19.18 kVA. For lower power values, sufficient shear strength was obtained, as well as aluminized unaffected coating on the entire surface of the welded point, which ensures good corrosion protection.

ACKNOWLEDGEMENTS

The research was sponsored by the Executive Agency for Higher Education, Research, Development, and Innovation (CNCS CCDI - UEFISCDI), within the framework of grant project Ref. PN-III-P2-2.1-PED-2019-3953/514PED 2019 - New composite material with ceramic layers deposited by laser processing for applications at high temperatures and corrosion – LASCERHEA, within PNCDI III.

REFERENCES

[1] **Sun X.**, *Effect of Projection Height on Projection Collapse and Nugget Formation - A Finite Element Study*, Welding Research Supplement, pp. 211-s to 216-s, 2001.

[2] **Gould J. E.**, *Challenges and Advances in Resistance Spot Welding Aluminium Sheet*, Resistance and Solid-State Welding. Edison Welding Institute, EWI, 28 April, 2014.

[2] **Wang X., Zhang Y.**, *Effects of Welding Procedures on Resistance Projection Welding of Nuts to Sheets*, ISIJ International, vol. 57, iss. 12, pp. 2194–2200, 2017.

[3] **Huang H. Y., Tseng K. H.**, *Process Parameters in Resistance Projection Welding for Optical Transmission Device Package*, Journal of Materials Engineering and Performance, vol. 20, iss. 2, pp. 244-249, 2011.

[4] **Han G., Ha, S., Marimuthu K. P., Murugan S. P., Park Y., Lee H.,** *Shape optimization of square weld nut in projection welding*, The International Journal of Advanced Manufacturing Technology, iss. 7-8, 2021.

[5] **Koal J., Baumgarten M., Heilmann S., Zschetzsche J., Füssel U**., *Performing an Indirect Coupled Numerical Simulation for Capacitor Discharge Welding of Aluminium Components*. Processes, vol. 8, 1330, doi:10.3390/pr81113302020, 2020.

[6] **Song Q.**, Testing and Modeling of Contact Problems in Resistance Welding, Ph.D Thesis, Technical University of Denmark, Kongens Lyngby, Denmark, 2003.

[7] **Pakala H**., *An investigation into the processes of projection welding of galvanized sheet*, Welding International, vol. 10, iss. 1, pp.5-13, 2009.

[8] **Vedani M**., *Microstructural and mechanical properties of stainless steel electrical resistance projection welds*. Welding International, vol. 16, iss. 9, pp. 696-703, 2002.

[9] **Voiculescu I**., **Geanta V., Vasile I. M., Ştefanoiu R., Iacob, M**., *Research regarding the obtaining of the electrode for spot welding*, Metalurgia International, Special Issue, no. 1, pp. 52-55, 2013.

[10] **Ceorapin C. G., Iovanas R., Voiculescu I**., **Iovanas D. M, Pascu A**., *Spot Welding Electrodes with the Active Area Achieved by Cladding with MMA Welding***,** Book Series: Annals of DAAAM and Proceedings, vol. 20, pp. 1361-1362, 2009.

[11] **Enrique P. D., Al Momani H., DiGiovanni Ch., Jiao Z., Chan K. R., Zhou N. Y.**, *Evaluation of Electrode Degradation and Projection Weld Strength in the Joining of Steel Nuts to Galvanized Advanced High Strength Steel*, J. Manuf. Sci. Eng., vol. 141(10): 104501, 8 pages, 2019.

[12] **Saha D. C., Park Y. D.**, *A Review on Al-Al/Al-Steel Resistance Spot Welding Technologies for Light Weight Vehicles*, *Journal of KWJS*, vol. 29, no. 4, pp. 397-40, 2011.

[13] **Zhang W. H., Qiu X. M., Sun D. Q., Han L. J.**, *Effects of resistance spot welding parameters on microstructures and mechanical properties of dissimilar material joints of galvanised high strength steel and aluminium alloy*, Science and Technology of Welding and Joining, vol. 16, iss. 2, pp. 153-161, 2011.

[14] **Spinella D. J., Van Otteren R., Borsenik B., Patrick E. P.,** *Single-Sided Projection Welding of Aluminum Automotive Sheet Using the HY-PAK ® Welding Process,* Journal of Materials & Manufacturing, SAE Transactions, vol. 109, sec. 5, pp. 963-969, 2000.

[15] **Gullino A., Matteis P., D'Aiuto F.**, *Review of Aluminum-To-Steel Welding Technologies for Car-Body Applications*, Metals, vol. 9, iss. 315, doi:10.3390/met9030315, 2019.

[16] **Huang H. Y., Tseng K. H.**, *Resistance projection welding for TO-Can style package* [J]. Acta Metallurgica Sinica (English Letters), vol. 22, iss. 4, pp. 255-262, 2009.

[17] **Miyamoto K., Nakagawa S., Sugi C., Sakurai H**. et al., *Dissimilar Joining of Aluminum Alloy and Steel by Resistance Spot Welding, SAE Int. J. Mater. Manf.*, vol. 2, iss. 1, pp. 58-67, 2009.

[18] **Taufiqurrahman I., Ahmad A., Mustapha M., Ginta T. L., Haryoko L. A. F., Shozib I. A.**, *The Effect of Welding Current and Electrode Force on the Heat Input, Weld Diameter, and Physical and Mechanical Properties of SS316L/Ti6Al4V Dissimilar Resistance Spot Welding with Aluminum Interlayer*, Materials, vol. 14, iss. 1129. https://doi.org/10.3390/ma14051129, 2021.

[19] **Yutanorm W., Juijerm P.**, *Diffusion enhancement of low-temperature pack aluminizing on austenitic stainless steel AISI 304 by deep rolling process*, Kovove Materialy, vol. 54, iss. 4, pp. 227–232, 2016.

[20] **Raut M., Achwal V**., *Optimization of Spot Welding Process Parameters for Maximum Tensile Strength*, Int. J. Mech. Eng. & Rob. Res., vol. 3, no. 4, pp. 506- 517, 2014.

[21] **Seikh A. H., Baig M., Singh J. K., Mohammed J. A., Luqman M., Abdo, H. S., Khan A. R., Alharthi N. H**., *Microstructural and Corrosion Characteristics of Al-Fe Alloys Produced by High-Frequency Induction-Sintering Process*, Coatings, vol. 9, iss. 686; doi:10.3390/coatings9100686, 2019.

[22] **Costa H. R. M**., **Dias J.S., Aguiar R. A. A., Lima R. A. A., Lopes D. M. M.**, *The effect of process parameters on the lifetime of copper electrodes used in spot welding of interstitial free steel sheets*, Annals of "Dunarea de Jos" University, Fascicle XII Welding Equipment and Technology, vol. 27, pp. 55-61, 2016.

[23] **Rosenthal I., Stern A.**, *Heat treatment investigation of the AlSi10Mg alloy produced by selective laser melting (SLM): microstructure and hardness*, Annals of "Dunarea de Jos" University, Fascicle XII Welding Equipment and Technology, vol. 27, pp.7-11, 2016.